



Proposal of Algorithm for 3D Object Detection of Obstacle Using Monocular Camera and Laser

Hayato Mitsuhashi and Taku Itami*

Department of Electrical Engineering, Graduate School of Science and Engineering, Meiji University, Ikuta, Japan

Submission: April 16, 2024; Published: April 23, 2024

*Corresponding author: Taku Itami, Department of Electronics and Bioinformatics, School of Science and Engineering, Meiji University, Ikuta, Japan

Abstract

In this study, we focused on obstacle distance measurement using a monocular camera and a cross laser, and proposed and validated an algorithm that can measure the depth of obstacles. Specifically, we proposed a real time distance measurement algorithm using a monocular camera and a cross laser that can be applied even in dark environments and can detect the depth of an obstacle by calculating the distance from the robot to the obstacle and the height of the obstacle. Algorithms that enable 3D object analysis of obstacles using only a camera and laser have not yet been studied. Furthermore, we confirmed the effectiveness of the proposed method by using two methods. First, the depth of the obstacle was calculated when the angle of the obstacle facing the robot was changed. Second, the depth of the obstacle was calculated when the robot moved horizontally parallel from the obstacle in front of it. As a result, the depth of the obstacle was accurately detected except when the placement angle of the obstacle in front was 0° or 90° . Furthermore, the depth of the obstacle was accurately detected when the robot moved horizontally parallel to the obstacle in front by 200 mm or more.

Keywords: Depth of obstacle; Realtime; Laser; Monocular camera; Disaster relief robot

Introduction

Natural disasters are increasing year by year in many parts of the world and are a major obstacle to a sustainable society. Every year, approximately 160 million people are affected worldwide, with about 100,000 lives lost and more than US\$40 billion in damages incurred [1]. Compared to the rest of the world, the Japanese archipelago is particularly prone to disasters [2]. For example, Japan experienced the Great Hanshin-Awaji Earthquake in January 1995, the Great East Japan Earthquake in March 2011, Typhoon No. 12 in September 2011, the landslide disaster in Hiroshima City caused by heavy rain in August 2014, the eruption of Mt [3].

When a disaster strikes, saving the lives of disaster victims is one of the highest priority issues [4]. The time from the occurrence of a disaster to the rescue is strongly related to the percentage of survivors among disaster victims [5]. Furthermore, according to the damage assumption of an earthquake directly under the Tokyo metropolitan area, the number of people who have difficulty in escaping by themselves due to building damage caused by shaking is estimated to be up to 72,000 for the entire affected area, making disaster mitigation measures and disaster

response capabilities that meet local conditions an urgent need [6]. When a disaster strikes, it is difficult to immediately prepare a large number of human resources to rescue people from the chaos. In addition, there are many situations in which it is difficult for humans to directly confirm the location of a disaster. To solve these problems, disaster rescue robots that can run autonomously are expected to play an active role [7,8,9]. Furthermore, in addition to lifesaving, autonomous mobile robots are required to increase performance, lower risks, lower costs, and improve efficiency in tasks such as firefighting, restoration work, and preventive inspections [10]. Focusing on obstacle detection methods, which are one of the key technologies for autonomous driving, stereo cameras, millimeter wave radar, and LiDAR have been actively studied [11,12,13]. However, there are limitations in terms of cost, size, and power consumption when considering their use in disaster rescue robots. Stereo cameras, one of the obstacle detection methods, have been used for obstacle detection in automobiles, and it is a highly practical method. However, when using ordinary cameras, spatial recognition in the dark is difficult. In the event of a disaster, the camera may be required to work in the dark because the outside light is blocked by debris and other

obstacles. Another disadvantage is that the processing cost and hardware cost are twice that of a monocular camera [14]. The mechanical LiDAR, which is currently the mainstream, requires a rotating mirror to be mounted on the housing due to its structure, and there are still concerns about the system size and durability for use in disaster relief sites [14].

On the other hand, research on obstacle distance measurement using a cross laser and a monocular camera has been conducted [15,16,17,18]. This method has advantages over the aforementioned sensors in terms of durability, sensor unit cost, and processing cost, but it has not yet been put into practical use. This method is currently capable of measuring the distance to an obstacle as well as the height and width of the obstacle, but has not yet reached the stage where it can detect the depth of the obstacle. When an obstacle suddenly appears in the robot's autonomous path finding, the robot can detect the distance to avoid the obstacle from the width of the obstacle but cannot calculate the distance to go straight to the back of the obstacle because the depth of the obstacle is undetectable [19]. In addition, the depth detection method using stereo cameras with machine learning is difficult to measure in dark environments, and the processing speed is slow. Although it is possible to easily detect the depth of obstacles by increasing the number of cameras or using LIDAR measurements, there are still issues to be solved in terms of cost and high computational complexity.

Therefore, we propose an algorithm that can detect the depth of obstacles using a monocular camera and a cross laser. Specifically, when the robot moves a small section parallel to an obstacle in front of it or changes the angle of the obstacle, the depth of the obstacle in the camera image can be accurately calculated by detecting the laser light at the depth of the obstacle using a binarization process and converting the distance using a cosine function.

The effectiveness of the proposed method is evaluated by calculating the depth of obstacles in front of the robot when the placement angle of the obstacles is changed and when the robot is moved horizontally.

Algorithm for calculating the depth of obstacle

In this research, a monocular camera reads the laser beam obtained by irradiating a green cross laser in the straight-ahead direction and analyzes the image information. The distance to the obstacle is calculated based on the similarity of triangles by detecting the position of the cross-laser light irradiated to the obstacle through image analysis [19]. The depth of the obstacle is calculated by the difference between the position of the laser light in the depth part acquired by the camera image and the linear distance of the front part of the obstacle.

Figure 1 shows a schematic representation of the experimental environment from the right side, showing each parameter. The height of the cross laser is H [mm], the height of the camera is

C [mm], and the maximum exposure distance is L [mm]. Let T_{max} [mm] be the maximum shooting range of the camera at the maximum irradiation distance of the cross laser, and t_m [pixel] be the pixel value in the image. Let the obstacle be placed in the straight ahead direction of the robot, the height TR [mm] of the irradiation position where the cross laser is projected onto the obstacle, and the pixel value t [pixel] at that position, then the height TR [mm] of the laser irradiation position can be obtained using the equation (1). The x-axis is the horizontal direction of the camera image, and the y-axis is the vertical direction. The pixel value t of the irradiated position can be calculated in real time by extracting the y-coordinate of the irradiated cross laser from the camera image. The height of the obstacle can be detected if t can be calculated, and the distance to the obstacle can be calculated based on the similarity of the triangles.

$$T_R = \frac{T_{max} \times t}{t_m} \quad (1)$$

From the above equation, the distance D [mm] from the obstacle can be obtained from the trigonometric ratio using equation (2).

$$D = L - \frac{T_R \times L}{H} \quad (2)$$

Figure 2 shows an image of the binarization flow, an image processing method used to calculate the height of obstacles and distance to obstacles. The frame width of the camera image is 320×240 [pixel]. Next, the entire frame was divided into 4×8 [pixel] segments. Then, 8 [pixel] is considered as one row, and the color closest to the green laser light is extracted for each row. Thus, 320 [pixel]/ 8 [pixel] = 40 rows were repeated. As described above, only the laser light can be extracted more accurately than by binarizing the entire frame at once. After the laser light was extracted, the image was repeatedly compressed and expanded using a kernel transformation to obtain a binarized image. The above method enables accurate binarization as a single line, even when the laser light extraction points are irregular or slightly separated from each other in neighboring rows. Accurate extraction of the laser light in the camera image affects the measurement accuracy.

The above methods calculated the straight line distance to the obstacle and the height of the obstacle. However, a method to calculate the depth of an obstacle using a monocular camera and a cross laser has not been developed. In the proposed method, we propose an algorithm to calculate the depth of an obstacle using only a monocular camera and a cross laser. When a robot repeatedly searches for a route to a destination in the event of disasters such as earthquakes and fires, it may be possible to create a new route if it can detect the depth of obstacles that appear unexpectedly in unexpected locations. To verify the effectiveness of an algorithm that can detect the depth of obstacles using a monocular camera

and a cross laser, the shape of the obstacle was chosen to be a simple object.

Figure 3 shows the camera image and top view of the robot when it faces an obstacle. The depth detection methods are shown for triangular and rectangular obstacles, respectively, and are compared in an environment where the initial positions of the obstacle and the robot are shifted to the front or side. The measurement condition is that even a small portion of the

depth of the obstacle is visible in the camera image. The distance calculated by the proposed method is not the direct distance from the camera, but the linear distance from the position where the camera is moved horizontally parallel to the obstacle in front of the robot. Therefore, if the position of the lowest point of the depth part of the obstacle captured by the camera can be confirmed in the binarized image, the depth of the obstacle can be calculated by the difference between the distance from the robot to the obstacle in the front part.

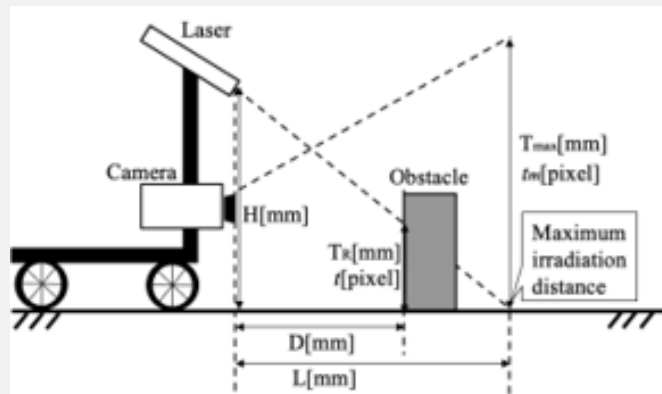


Figure 1: Environment for calculating distance and height to obstacles by triangulation (Detects the distance and height of obstacles from the height and angle of the camera and laser.).

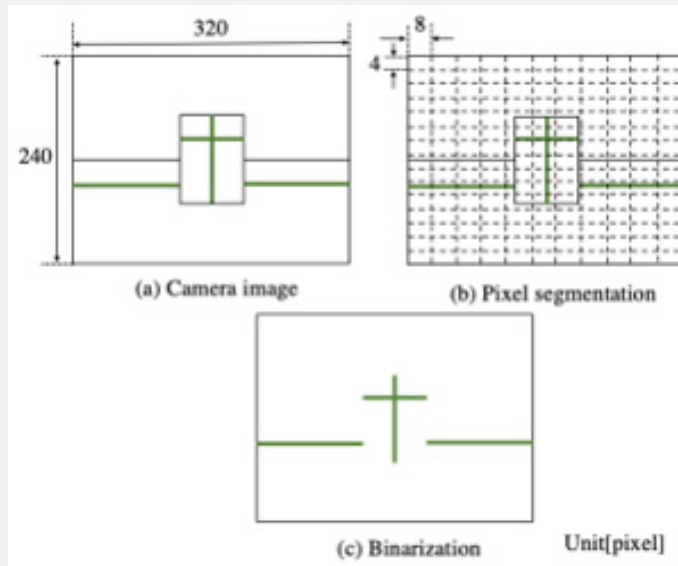


Figure 2: Diagram of the binarization flow (First, divide the 320 x 240 pixels into 8 x 4 pixels. Here, 8x4 pixels are considered to be 1 pixel. Next, the color closest to the laser beam is extracted for each row. In other words, there are 40 columns in total, and 40 pixels with colors similar to laser light are extracted.).

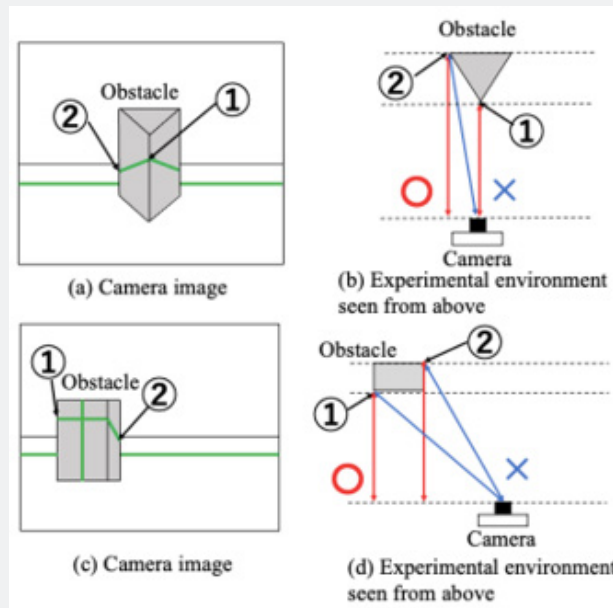


Figure 3: Camera image and top view of the robot facing an obstacle (The distance calculation method in this proposed method does not calculate the straight-line distance from the camera. The distance calculation in this proposed method calculates the straight-line distance from the position where the camera is translated horizontally. Therefore, it is possible to accurately detect the depth of the obstacle.).

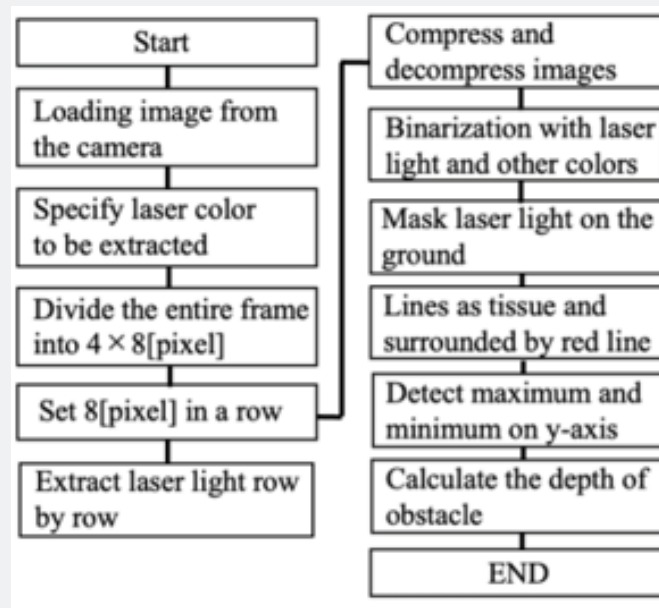


Figure 4: Flowchart of binarization (The distance to the obstacle in this proposed method is calculated using real-time processing. Distance information can be calculated at 0.5 second intervals.).

The flowchart of the proposed method is shown in Figure 4. First, the threshold range of laser color is set in advance and camera images are acquired. Next, a 320×240 [pixel] camera image is divided into 8×4 [pixel] rows, where each row is 8[pixel] and the color closest to the laser color is specified for each row. 40 rows

of the above process are repeated to binarize the camera image into the laser color and other colors. After acquiring the binarized image, the image is compressed and expanded repeatedly to transform the kernel in the camera image. Furthermore, the laser light on the ground is masked, so that only the laser light irradiated

on the obstacle is displayed. The laser position after binarization in the camera image and the linear distance from the position where the camera is moved horizontally parallel to the obstacle in front of the camera are calculated using Equation (1, 2). Next, the maximum and minimum positions in the y-axis direction of the laser beam irradiated on the obstacle are detected. The specific method for detecting the maximum and minimum positions is to recognize a set of connected lines and enclose the area of each set of lines with a red line. The upper part of the red line is recognized as the maximum position on the y-axis and the lower part as the minimum position on the y-axis. Finally, the depth of the obstacle is calculated by the difference between the maximum and minimum positions. As an example, the flow for calculating the depth length of an obstacle is shown in Figure 5. First, the camera image of the robot when it faces the obstacle is acquired. Next, the image is binarized, and the kernel transformation is used to organize the pixels in the laser beam area. Furthermore, as shown in (c), the straight lines that exist in the binarized image are recognized as a set and a red frame is provided. Finally, the distance from the camera to the obstacle in the frontal part is shown in the upper left corner, and the distance from the robot to the obstacle in the deepest part, which is farthest from the robot, is shown in the lower right corner. When the former is 300 mm and the latter is 350 mm, the depth of the obstacle can be detected to be 50 mm by the difference method.

Therefore, accurate recognition of the laser light by the binarized image is essential for the measurement accuracy of the proposed method. The flowchart of the proposed method is shown in Figure 4. First, the threshold range of laser color is set in advance and camera images are acquired. Next, a 320×240 [pixel] camera image is divided into 8×4 [pixel] rows, where each row is 8[pixel] and the color closest to the laser color is specified for

each row. 40 rows of the above process are repeated to binarize the camera image into the laser color and other colors. After acquiring the binarized image, the image is compressed and expanded repeatedly to transform the kernel in the camera image. Furthermore, the laser light on the ground is masked, so that only the laser light irradiated on the obstacle is displayed. The laser position after binarization in the camera image and the linear distance from the position where the camera is moved horizontally parallel to the obstacle in front of the camera are calculated using Equation (1, 2). Next, the maximum and minimum positions in the y-axis direction of the laser beam irradiated on the obstacle are detected. The specific method for detecting the maximum and minimum positions is to recognize a set of connected lines and enclose the area of each set of lines with a red line. The upper part of the red line is recognized as the maximum position on the y-axis and the lower part as the minimum position on the y-axis. Finally, the depth of the obstacle is calculated by the difference between the maximum and minimum positions. As an example, the flow for calculating the depth length of an obstacle is shown in Figure 5. First, the camera image of the robot when it faces the obstacle is acquired. Next, the image is binarized, and the kernel transformation is used to organize the pixels in the laser beam area. Furthermore, as shown in (c), the straight lines that exist in the binarized image are recognized as a set and a red frame is provided. Finally, the distance from the camera to the obstacle in the frontal part is shown in the upper left corner, and the distance from the robot to the obstacle in the deepest part, which is farthest from the robot, is shown in the lower right corner. When the former is 300 mm and the latter is 350 mm, the depth of the obstacle can be detected to be 50 mm by the difference method. Therefore, accurate recognition of the laser light by the binarized image is essential for the measurement accuracy of the proposed method. obstacle is 60 mm.

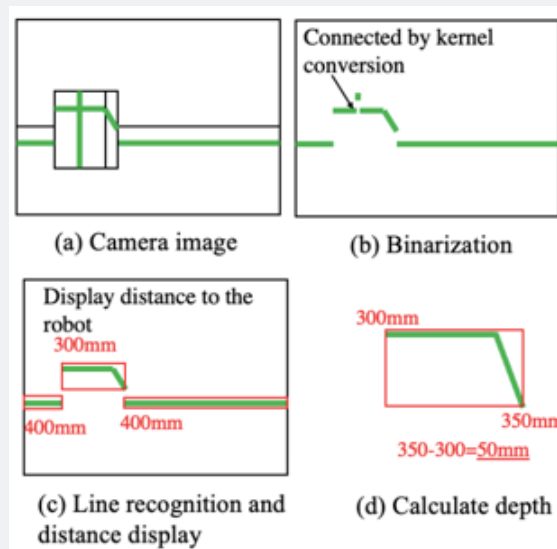


Figure 5: Flow of calculating depth length at obstacles (After detecting the laser through binarization processing, obtain the pixel coordinates within the frame. Next, calculate the distance to the obstacle using equations (1) and (2). The actual depth of the obstacle is calculated by subtracting the distance between the depth of the obstacle and the distance from the front of the obstacle.).

Next, the distance between the robot and the obstacle was set to 300 mm. One method calculates the depth of the obstacle by rotating the obstacle in front of the robot every 10 degrees. The second method calculates the depth of the obstacle when the robot moves horizontally parallel to the obstacle at 100 mm intervals from the obstacle in front of it. The four measurement points are when the robot is in front of the obstacle and when the robot translates 0, 100, 200, and 300 mm laterally from its initial position. The frontal point was defined as measurement environment 1, the 100 mm parallel shift as measurement environment 2, the 200 mm parallel shift as measurement environment 3, and the 300 mm parallel shift as measurement environment 4. The experiment was conducted indoors on a flat

floor.

Validation of effectiveness

In this study, the effectiveness of the proposed method was confirmed by two methods. First, the depth of the obstacle was calculated when the angle of the facing obstacle was changed. Second, the depth of the obstacle was calculated when the robot moved horizontally parallel from the obstacle in front of it. Figure 6 shows the experimental environment when the angle of the obstacle in front was changed, and Figure 7 shows the experimental environment when the robot moved horizontally parallel to the obstacle.

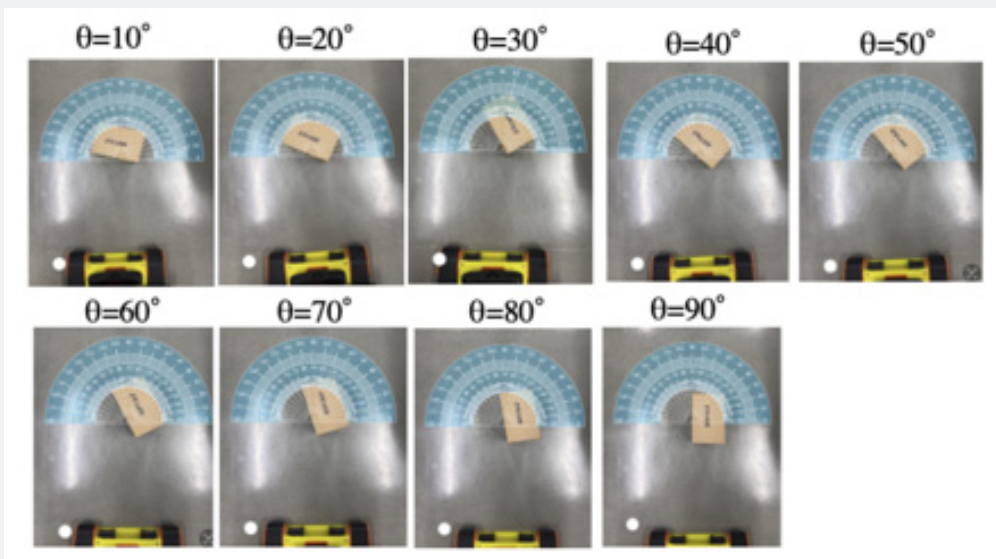


Figure 6: Obstacle placement angle viewed from above (The effectiveness of the proposed method is verified by changing the placement angle of obstacles in 10-degree increments.).

First, a rectangular brown paper box was prepared in the direction of the robot's straight ahead. The depth of Figure 8 and Figure 9 show the measurement results of calculating the depth of obstacles in the measurement environment 1-4 using the proposed method. Figure 11 shows the binarized image after kernel transformation. The upper figure in Figures 8 and 10 shows the distance from the robot to the front of the obstacle, and the lower figure shows the distance from the robot to the depth of the obstacle. Therefore, the depth of the obstacle can be calculated by subtracting the lower value from the upper value. The horizontal axis in Figure 8 shows the angle of the obstacle placement and the vertical axis shows the depth of the obstacle; the horizontal axis in Figure 9 shows the distance of the robot from the obstacle in front of it to a parallel position, and the vertical axis shows the depth of the obstacle. The depth lengths and errors of the obstacles for the experimental environment 1-4 are shown in Table 1.

Table 1: Depth length and error of obstacles relative to experimental environment 1-4 (It was confirmed that the depth of an obstacle could be detected with a maximum error of 4 mm from a position where the robot was moved horizontally by more than 100 mm toward the obstacle in front of it.).

Environment	Depth Length	Error
1	None	None
2	34	-26
3	64	+4
4	64	+4

The results of Figure 8 show that the robot was able to accurately calculate the depth of the obstacle between 20° and 60° when the obstacle was placed in front of the robot and the angle of placement was varied. When θ is 70° or 80°, the depth of the obstacle is calculated differently than when θ is between 20° and 60°, which may have caused the error.

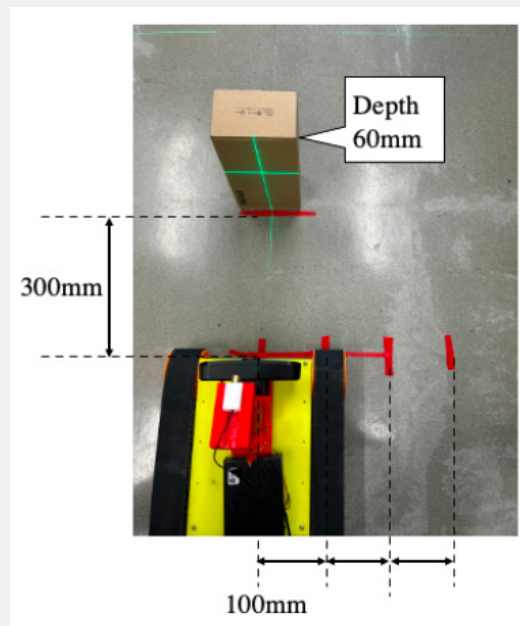


Figure 7: Actual measurement environment(In Figure 6, the placement angle of the obstacles was changed. In Figure 7, the robot is moved horizontally toward the obstacle in front of it. The effectiveness of the proposed method was verified by detecting the depth information of the obstacle from the moved position.).

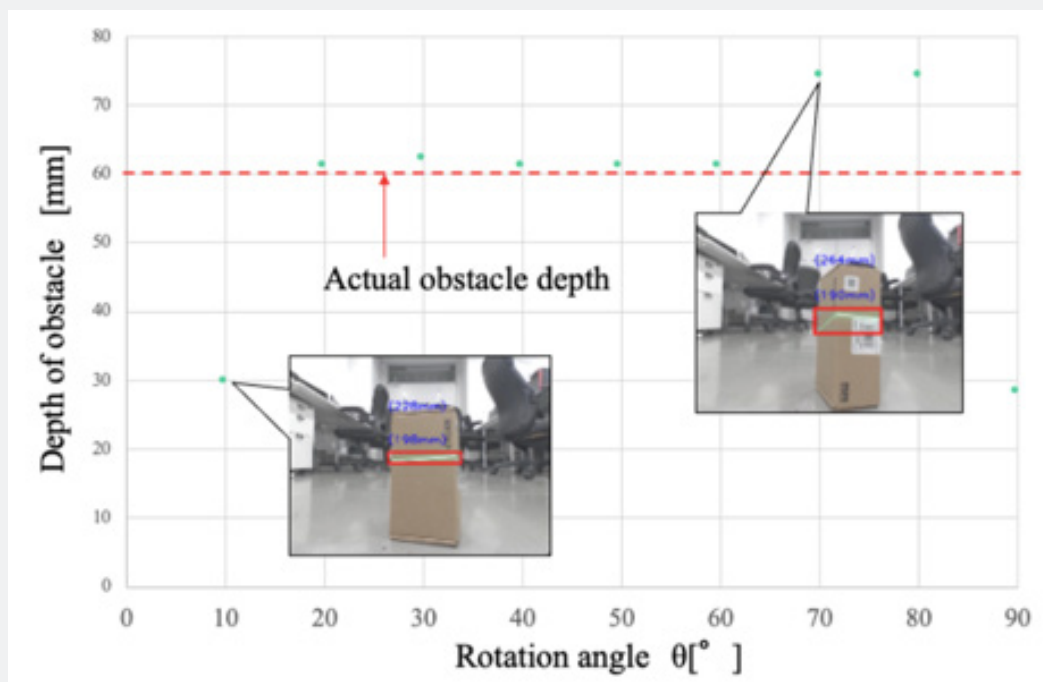


Figure 8: Depth of obstacle relative to angle of rotation of obstacle (The results of the proposed method are shown in Fig.6. The reason why there is a large error at 70 degrees and 80 degrees is because the depth length on the opposite side is detected. The depth on the opposite side is 75mm, so we confirmed that accurate detection was possible at all error of 4 mm from a position where the robot was moved horizontally by more than 100 mm toward the obstacle in front of it.).

As shown in Figure 9, it was difficult to detect the depth of the obstacle in measurement environment 1 when there was an obstacle in front of the robot, because the depth of the obstacle was not reflected in the camera image. In Environment 2, when the robot was moved 100 mm horizontally in parallel, the error

was 26 mm. In the case of measurement environments 3 and 4, in which the robot was moved 200 and 300 mm horizontally, the depth of the obstacle could be detected with an error of 4 mm.

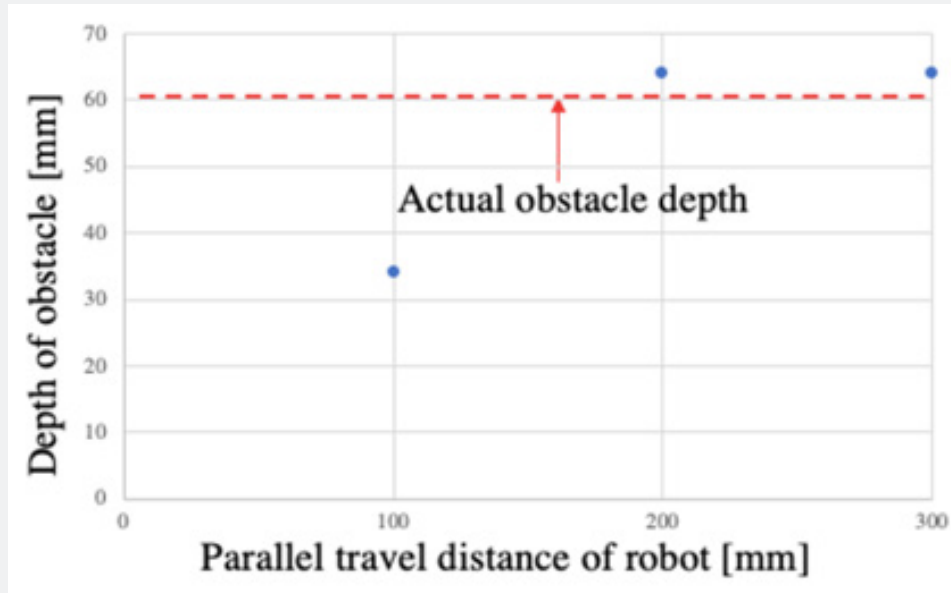


Figure 9: Depth of obstacle relative to distance when the robot moves horizontally parallel to it (The results of the proposed method are shown in Fig.7. It was confirmed that the depth of an obstacle could be calculated accurately when the robot was moved laterally for more than 100mm.).

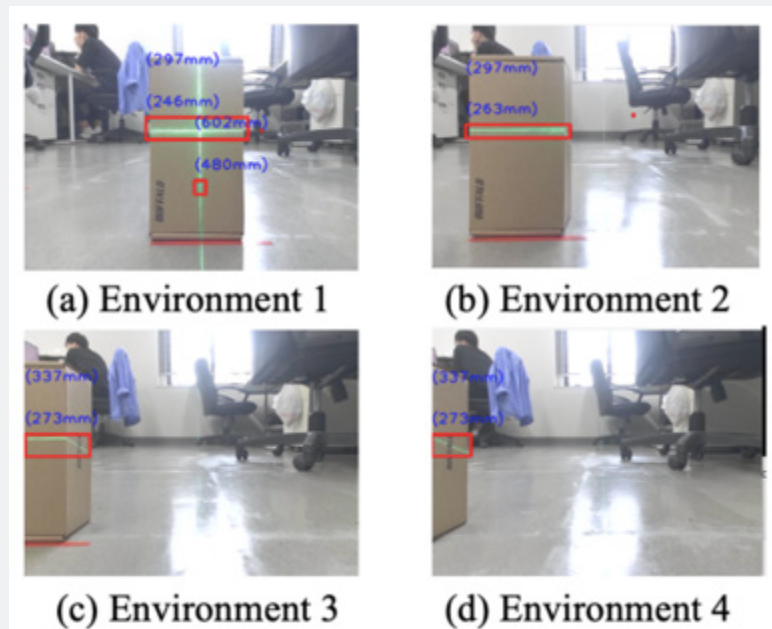


Figure 10: Camera image showing the distance from the robot to the obstacle (It was confirmed that the laser beam irradiated onto an obstacle could be accurately detected. Furthermore, by subtracting the two numbers in environments 2, 3, and 4, the depth of the obstacle can be calculated.).

From the camera images and the kernel transformed binary images shown in Figures 10 and 11, it was confirmed that the green laser light irradiated on the obstacle was accurately extracted. In addition, when an obstacle is placed in front of the robot, the depth of the obstacle cannot be detected because the depth of the obstacle is not reflected in the camera image. As shown in (d) of Figure 10, we confirmed that the depth of the obstacle can be detected accurately if the front and back parts of the obstacle can be seen in the camera image even a little.

Consideration

Figure 8 shows that the obstacle was placed in front of the robot and the depth of the obstacle was calculated with a maximum error of 3 mm for the range of θ from 20° to 60° by changing the placement angle. The reasons for the above results include the fact that the depth of the obstacle was captured in the camera image, the high accuracy of the binarization method that extracts only the laser light, and the accuracy of the formula used to calculate the depth of the obstacle in our proposed method. The reason for the large error in the depth of the obstacle when θ is 10° or 90° is considered to be that the depth of the obstacle is not fully captured in the camera image, and when θ is 70° or 80°, the

depth is calculated for a different portion than when θ is 20° to 60°. The proposed method is therefore more effective for frontal images. Therefore, we confirmed that the proposed method can accurately detect the depth of obstacles within the range of 20° to 80° when there is an obstacle in front of the camera.

Figure 9 shows that in measurement environment 1, where the obstacle is in front of the robot, it was difficult to detect the depth of the obstacle because the depth of the obstacle was not reflected in the camera image. In Environment 2, when the robot was moved horizontally by 100 mm, the error was 26 mm. In measurement environments 3 and 4, where the robot was moved 200 and 300 mm horizontally, the depth of the obstacle could be detected with an error of 4 mm. The reason why the depth of the obstacle could not be calculated accurately in measurement environment 2 is thought to be that the laser light in the depth area could not be accurately processed into a binary value. The kernel transformed binary image in Figure 11 confirms that the green laser light irradiating the obstacle was accurately extracted. The farther the distance is from the obstacle, the more difficult it is to recognize the laser light in the camera image. Therefore, it is necessary to accurately detect the laser light in the depth part of the obstacle to further improve the measurement accuracy.

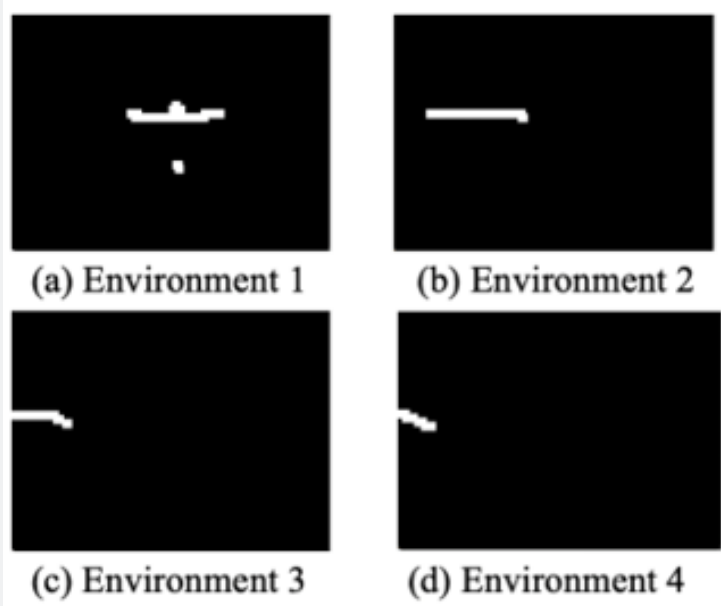


Figure 11: Binarized image after kernel conversion (We confirmed that laser light could be detected more accurately than binary video. One of the reasons why the depth of the obstacle could be calculated accurately is thought to be because this binarized image is accurate.).

Summary

In this study, we focused on obstacle distance measurement using a monocular camera and a cross laser, and proposed and verified an algorithm that can measure three dimensional objects.

Specifically, we proposed a real time distance measurement algorithm using a monocular camera and a cross laser that is not affected by the illumination of the measurement environment and can detect the depth of an obstacle by calculating the distance from the robot to the obstacle and the height of the obstacle.

Furthermore, we confirmed the effectiveness of the proposed method by using two methods. First, the depth of the obstacle was calculated when the angle of the obstacle facing the robot was changed. Second, the depth of the obstacle was calculated when the robot moved horizontally parallel from the obstacle in front of it. As a result, the depth of the obstacle was accurately detected except when the placement angle of the obstacle in front was 0° or 90°. The reason why the obstacle could not be detected accurately when the placement angle of the obstacle was 0° or 90° was because the depth of the obstacle was not fully captured in the camera image. Furthermore, the depth of the obstacle was accurately detected when the robot moved horizontally 200 mm or 300 mm from the obstacle in front of it. The reason for the error of 26 mm in the depth of the obstacle when the robot moved 100 mm horizontally is considered to be that the laser light in the depth part of the obstacle could not be accurately extracted when generating the binary image. The larger the distance from the robot, the more difficult it becomes to detect the laser light in the camera image. This is because the color of the laser light has the characteristic of changing slightly with distance. Therefore, we confirmed that the initial binarization threshold range must be set accurately so that the laser light can be acquired according to the distance from the robot.

The use of this autonomous mobile robot was limited to an environment with a smooth road surface to measure the depth of obstacles, so it is necessary to consider a robot that can be applied to cases where the robot cannot maintain a level surface. In order to verify the effectiveness of the proposed method, a rectangular shape, which is the simplest shape, was used as the obstacle shape in this measurement environment. However, in the event of a disaster, obstacles of various shapes are likely to exist in unexpected locations. Therefore, it is necessary to construct a system that can detect the depth of obstacles using the proposed method without being affected by the shape of the obstacles. If the proposed robot can be realized, it can be used as an autonomous mobile robot in the event of a disaster, and can respond to unexpected obstacles placed while traveling to a destination, because it can detect the depth of the obstacles. In recent years, methods for detecting the depth of obstacles have been proposed using camera-based deep learning, etc. However, since the proposed method uses a monocular camera and laser, it can detect obstacles without being affected by measured illumination, which is considered the greatest advantage of the proposed method.

References

1. Yengin H (2019) Research on Improvement of Logistics System Based on Analysis of Emergency Assistance Logistics System and Its Actual Operation during Disasters, Kyushu University Institutional Repository.
2. Scho Y (2019) What it means to live in the world's most disaster-prone country, Kobe University Ocean Bottom Exploration Center No. 136.
3. (2021) Institute of Okinawan Studies, Hosei University: Factors Contributing to the Extent of Damage in the Hanshin-Awaji Earthquake, Okinawa Journal of Geographical Studies No. 21, pp. 73-78.
4. Asama H (2012) Robot technology required for disaster and accident response, *Materia* 51(4): p. 140.
5. Chiu Y, Omura H, Chen H, Chen S (2020) Indicators for Post-Disaster Search and Rescue Efficiency Developed Using Progressive Death Tolls, *Sustainability* 2020 No. 12.
6. Suetsugu M, Yang S, S (2019) Serikawa Obstacle detection and shape recognition method for mobile robots using line laser and camera, *National Conference of the Society of Industrial and Applied Engineering* pp. 5-6
7. Kina K, Inagaki K, Sadohara S, Yashiro H (2020) An attempt of rescue capability evaluation considering regional characteristics, *Journal of the Architectural Institute of Japan* 85 (775) pp. 1955-1963.
8. Nakamura S, Xie M, Murata M, Mori T (2021) Acquisition of Multi-Agent Cooperative Behavior in Disaster Relief Problem Using NashQ Learning, *Information Processing Society of the Japan Kansai Branch, Collection of lectures.*
9. Sakaguchi N, K Ohno, Takeuchi E, Nagaya N, Tadokoro S (2013) Development of Long Term Usable and Search Recording Devices for Rescue Dogs, *Proceedings of the 2013 JSME Conference on Robotics and Mechatronics, Tsukuba, Japan, May 22-25.*
10. Shamsoshoara A, Afghah F, Razi A, Mousavi S, Ashdown J, et al. (2020) An Autonomous Spectrum Management Scheme for Unmanned Aerial Vehicle Networks in Disaster Relief Operations, *2020 IEEE International Conference on Acoustics* Vol. 8.
11. Tadokoro O (2019) Research on lifesaving robots for major disasters, *Journal of the Robotics Society of Japan* 37(9): pp. 789-794.
12. Zhai G, Zhang W, Hu W, Ji Z (2020) Coal Mine Rescue Robots Based on Binocular Vision, A Review of the State of the Art, *2020 IEEE International Conference on Acoustics* Vol. 8.
13. Faizan Khan M, Wang G, Zakirul Alam Bhuiyan MD (2019) Towards Debris Information Analysis and Abstraction for WiFi Radar Edge in Collapsed Structures, *2019 IEEE International Conference on Acoustics* Vol. 7.
14. Li M, Zhu H, you S, Wang L, Tang C (2019) Efficient Laser-Based 3D Slam for Coal Mine Rescue Robots, *2019 IEEE International Conference on Acoustics* Vol. 7.
15. Suetsugu M, Yang S, Serikawa Kyushu S (2019) Institute of Technology Mobile robot using line laser and camera Obstacle detection and shape recognition method, *Proceedings of IIAE Annual Conference 2019, September 18-20.*
16. Totoki S, Akamine S, Kobayashi S, Itami T, Yoneyama J (2022) Realtime dynamic obstacle detection using a line laser and camera in the dark, *AROB 27th.*
17. Mitsuhashi H, Kobayashi S, Akamine S, Itami T, Yoneyama J (2022) Realtime Distance Measurement Algorithm with Automatically Determinable Threshold Value Using a Monocular Camera and Line Laser, *SICE Annual Conference 2022, September 6-9.*
18. Mitsuhashi H, Akamine S, Itami T, Yoneyama J (2023) Autonomous Mobile Robot Equipped with a Monocular Camera and Crossed Laser that can Measure Obstacle Distance in Real Time Independent of Brightness, *31st Mediterranean Conference on Control and Automation (MED)*
19. Akamine S, Itami T, Yoneyama J (2022) Realtime Obstacle Detection in a Darkroom Using a Monocular Camera and a Line Laser, *Journal of the International Society of Artificial Life and Robotics (ISAROB).*



This work is licensed under Creative Commons Attribution 4.0 License
DOI: [10.19080/RAEJ.2024.06.555676](https://doi.org/10.19080/RAEJ.2024.06.555676)

**Your next submission with Juniper Publishers
will reach you the below assets**

- Quality Editorial service
- Swift Peer Review
- Reprints availability
- E-prints Service
- Manuscript Podcast for convenient understanding
- Global attainment for your research
- Manuscript accessibility in different formats
(Pdf, E-pub, Full Text, Audio)
- Unceasing customer service

Track the below URL for one-step submission
<https://juniperpublishers.com/online-submission.php>